



Published in final edited form as:

J Orthop Res. 2007 May ; 25(5): 646–655.

AGE-RELATED FACTORS AFFECTING THE POST-YIELD ENERGY DISSIPATION OF HUMAN CORTICAL BONE

Jeffrey S. Nyman¹, Anuradha Roy², Jerrod H. Tyler¹, Rae L. Acuna¹, Heather J. Gayle¹, and Xiaodu Wang¹

1Department of Mechanical Engineering and Biomechanics The University of Texas at San Antonio San Antonio, Texas 78249

2Department of Management Science and Statistics The University of Texas at San Antonio San Antonio, Texas 78249

Abstract

The risk of bone fracture depends in part on the quality of the tissue, not just the size and mass. This study assessed the post-yield energy dissipation of cortical bone in tension as a function of age and composition. Tensile specimens were prepared from tibiae of human cadavers in which male and female donors were divided into two age groups: middle aged (51 to 56 years old, $n = 9$) and elderly (72 to 90 years old, $n = 8$). By loading, unloading, and reloading a specimen with rest period inserted in between, tensile properties at incremental strain levels were assessed. In addition, the post-yield toughness was estimated and partitioned as follows: plastic strain energy related to permanent deformation, released elastic strain energy related to stiffness loss, and hysteresis energy related to viscous behavior. Porosity, mineral and collagen content, and collagen crosslinks of each specimen were also measured to determine the micro and ultrastructural properties of the tissue. It was found that age affected all the energy terms plus strength but not elastic stiffness. The post-yield energy terms were correlated with porosity, pentosidine (a marker of non-enzymatic crosslinks), and collagen content, all of which significantly varied with age. General linear models with the highest possible R^2 value suggested that the pentosidine concentration and collagen content provided the best explanation of the age-related decrease in the post-yield energy dissipation of bone. Among them, pentosidine concentration had the greatest contribution to plastic strain energy and was the best explanatory variable of damage accumulation.

Keywords

bone; porosity; collagen; pentosidine; toughness

INTRODUCTION

There has been growing awareness that additional factors beyond bone size, mass, and density are important to the changes that make the skeleton more susceptible to fracture with age.¹⁻³ Measurements of bone mineral density (BMD) and structural geometry of the hip by X-ray absorptiometry are useful in assessing fracture risk.⁴⁻⁶ However, such measurements do not necessarily indicate that bone fracture is imminent.^{7, 8} Although BMD can be measured noninvasively and is highly correlated with bone strength,⁹⁻¹¹ it does not necessarily characterize bone quality or specifically the inherent integrity of the extracellular matrix of bone tissue. Clinical observation has revealed that similar postmenopausal loss of bone mass occurs in Giambian and Chinese women as does their Caucasian counterparts, but the fracture

incidence is much lower.^{12, 13} Moreover, the probability of fracture increases with age independent of BMD.^{14, 15} Thus, there seem to be other age-related changes influencing the resistance of bone to fracture. In fact, previous studies have suggested a number of possible changes that may affect the mechanical competence of bone in terms of the morphology and the extracellular matrix of cortical bone (Table 1).

As an informative measure of bone quality, toughness has been observed to decrease with age when measured by the area under a stress-strain or force-displacement curve generated by monotonically loading *ex vivo* bone specimens in tension^{16, 17} or bending^{18, 19}, respectively. Decreases in critical strain energy release rate (G_{Ic}) and stress intensity factor (K_{Ic}), two measures of fracture toughness, have also indicated that aged cortical bone is less resistance to crack initiation and propagation.^{18, 20-25} Perhaps more importantly, aging decreases the normal rise in crack growth resistance as a crack extends (i.e., there is a decrease in the slope of the R-curve or K_I vs. crack length).^{26, 27} This suggests that age affects the toughening mechanisms of bone.

Being an inhomogeneous material with a highly hierarchical structure, bone's resistance to failure cannot fully be characterized by material properties like G_{Ic} and K_{Ic} , which are derived using linear elastic fracture mechanics.²⁸ One complementary approach is to analyze post-yield energy dissipation through multiple, progressive cycles of deformation. Much of the toughness of bone occurs after yielding, and energy depends on both the strength and ductility (i.e., degree of permanent deformation) of bone.

Based on earlier studies that examined the effect of overloading (damaging) on bone's mechanical behavior,²⁹⁻³¹ we recently developed a loading-rest-unloading-rest-reloading protocol for tension that partitions energy dissipation into three components: released elastic strain energy related to stiffness loss, hysteresis energy related to viscous deformation, and plastic strain energy related to permanent deformation.³² The potential advantage of this test over monotonic loading is the acquisition of multiple mechanical properties over increasing degrees of yielding to provide insights into failure mechanisms of bone. Using this new protocol, we intended to investigate in the present study the age-related effect on the characteristics of post-yield energy dissipation. In addition, we measured porosity, collagen crosslink concentrations, collagen content, mineral and organic fractions, tissue density, and water content of cortical bone from the anterior quadrant of the tibia. Hypothesizing that ultrastructural changes are the best explanatory variable of post-yield energy dissipation, we investigated whether age affected these compositional and morphological properties of bone and whether they correlated with the mechanical properties.

MATERIALS AND METHODS

Specimen Preparation

Seventeen human tibiae each produced one tensile cortical bone specimen ('Dog bone' type). The Willed Body Program (The University of Texas Southwestern Medical Center at Dallas, TX) supplied the cadaveric tissue under stipulation that the donors had no known bone disease. Donors were divided into two age groups: (a) the middle aged group (Mid: n=9) included four females with ages of 53, 54, 54, and 56 years and five males with ages of 49, 51, 51, 52, and 55 years while (b) the elderly group (Old: n=8) included four females with ages of 84, 88, 88, and 90 years and four males with ages of 72, 76, 79, and 87 years. Using a circular, diamond saw (Isomet 2000, Buehler, Lake Bluff, IL), an axial bone strip with a nominal thickness of 2.3 mm was collected from the anterior aspect (*i.e.*, longitudinally oriented osteons) of the mid-diaphysis. The strip was milled by a CNC machine (ProLIGHT 1000, Light Machines, Manchester, NH) into a tensile specimen (the grip regions were 10 mm × 5 mm; the gage region

was 10 mm × 2 mm; and the tapers were 10 mm long with a fillet radius of 20 mm). Specimens were wrapped in gauze soaked in phosphate buffered saline and stored at −20 °C until testing.

Mechanical Testing

A bench-top mechanical testing system (EnduraTEC Elf 3300, Bose Corporation, Minnetonka, MN) was used to conduct post-yield tests in tension with a multiple loading-unloading-reloading scheme. The loading protocol was: 1) load specimen in displacement control to an initial level of 0.05 mm, 2) hold the displacement at the level of 0.05 mm for 30 seconds (stress relaxation), 3) unload in force control to zero force, 4) hold for 30 seconds at zero force (anelastic relaxation), and 5) reload in displacement control to the next displacement level with an increment of 0.05 mm. This procedure was repeated iteratively until failure (Fig. 1B). The dwell periods provided a quasi-equilibrium condition for measuring stiffness loss. Our preliminary tests indicated that a thirty second period of rest for the dwell was long enough to accommodate stress changes caused by the viscoelastic behavior for both the undamaged (within the elastic range) and damaged (post-yield) tissue. The loading and unloading rates were 0.5 mm/min and 480 N/min, respectively, to ensure a consistent strain rate during loading. Strain was recorded with an extensometer (MTS 632.26F-20, 8 mm gage, Eden Prairie, MN) to produce engineering stress versus engineering strain curve (Fig 1). Ultrapure water dripped on the specimen at a nominal rate of 4 mL/min throughout the mechanical testing to keep it hydrated.

Quantification of Energy Dissipation

Post-yield energy dissipation of bone was partitioned as shown in Fig. 1 and as described by Wang and Nyman.³² Briefly, the released elastic strain energy (U_{er}) was quantified as the area under the last unloading curve on a stress-strain plot before failure minus the recovered elastic strain energy (U_{e0} or the area enclosed by the curves connecting at *c*, *d*, and *e*). The irreversible energy consumption (U_m) was quantified as the area between successive loading curves (*e.g.*, between curve *a* to *b* and curve *g* to *h*) on the stress-strain plot. It is noteworthy that U_m accumulates with each bout of loading (Fig. 1B). Plastic strain energy (U_{ps}) was quantified as the difference between the accumulated, irreversible energy consumption

($U_m = \sum_{i=1}^{C_f} U_i$) and the U_{er} at the last cycle before failure ($U_{ps} = U_m - U_{er}$). Here, C_f is number of cycles before failure, and U_i is the energy loss between successive reloading curves. The measure of viscoelastic/plastic energy dissipation, known as hysteresis energy (U_h), was quantified as the area between the unloading, rest, and reloading curves of the last cycle before failure (*e.g.*, between curve *c* to *f* and curve *g* to *h*).

In addition to the individual energy dissipation terms, the complete energy dissipated before failure was also quantified. This energy is akin to the toughness (U_T) of bone and was equal to the sum of U_m , U_h , U_{er} , U_{e0} , and the final energy (U_f). The latter is the area enclosed by curves connected at *d*, *c*, *h*, *i*, and *j* (Fig. 1A)

For the most complete characterization of post-yield energy behavior, specimens must break after the stress returns to the dwell stage of the last cycle (point *h* in Fig 1A). However, most specimens broke after passing this strain but before the next loading cycle. The question then arose of whether this underestimation of energy is greater in one age group than the other and cause misleading interpretation of the data. To quantify the degree of underestimating the post-yield energy terms (U_{ps} , U_{er} , and U_h), the energy (U_f) dissipated from the last dwell strain until failure was calculated. Fortunately, there were no statistically significant differences in this underestimation between middle and old bone specimens in the present loading scheme. Without strict strain control, deformation can sometimes occur in the gage region when the movement of the actuator is halted. Thus, the strain difference between the start and end of the

first dwell (stress relaxation) was summed over the cycles for each specimen. This unintended cumulative deformation did not vary between the age groups, suggesting that any unquantifiable damage mechanism caused by the use of displacement control did not unduly contribute to the age-related differences in mechanical properties.

Quantification of Strength, Elastic modulus, and Damage

The maximum stress (σ_{\max}) was recorded from each stress-strain plot and served as the strength characteristic of the tensile specimen. The elastic modulus was estimated from the initial, linear loading curve on the stress-strain plot (*i.e.*, E_0 in Fig. 1). All mechanical properties were calculated using a numerical analysis programmed in Matlab (v7.0.1, The Mathworks, Inc., Natick, MA). Age differences in final damage density was also investigated by estimating the linear measure of stiffness loss

$$D_f = 1 - \frac{E_i}{E_0} \quad (1)$$

where E_i is the elastic modulus at the last cycle of loading and E_0 is the initial elastic modulus of bone.³³ E_i was calculated as the slope between the relaxation points on the stress-strain curve (between *c* and *g* in Fig. 1).

Porosity Measurement

A cross-section, 1 mm in thickness, near the broken surface of tensile specimen was removed with a diamond, circular saw from each specimen. After grinding the fracture surface by hand with successive grits of silicon carbide paper (600, 1200, 2400, 4000) and 0.05 μ alumina solution, the aerial porosity of Haversian canals and resorption spaces in each cross-section was quantified by converting digital images into binary form as describe previously.³⁴ To eliminate bias, three users, who were blind to the age of the donor, independently processed and calculated porosity (P_o), which is the black area divided by total area and expressed as a percentage. The mean value was used in the statistical analysis.

Gravimetric measurements

The other half of the broken tensile specimen was weighed with an electronic balance (PB303-S, Mettler Toledo, Greifensee, Switzerland) while submerged in water and then while in air (after lightly blotting). Specimens were dried at 102 °C in a vacuum oven (25 in Hg) for forty hours and ashed at 600 °C in a furnace (FB1300, Barnstead International, Dubuque, IA) for twenty-four hours. Dividing the wet mass of bone by the volume of bone as determined by Archimedes principle provided a measure of the apparent density of wet bone tissue (ρ_b). Likewise, dividing the mineral mass by the volume of the mineral phase provided the apparent density of bone mineral (ρ_m). Lastly, dividing the loss of mass due to drying (at 102 °C) by the volume of bone provided water content (ΔH_2O). We calculated organic fraction as organic mass per wet bone mass (M_{Org}/M_{wet}), but the mineral fraction as mineral mass per dry bone mass (M_{Min}/M_{dry}) because, unlike M_{Org}/M_{wet} , M_{Min}/M_{wet} was correlated to porosity ($\rho_{xy} = 0.694$; p -value = 0.002) negating its meaningfulness. The ratio of mineral mass per organic mass (M_{Min}/M_{Org}) was also calculated.

Crosslink Measurements

From each tensile specimen, a small piece of bone was cut from the corner of the grip region to measure the concentration of hydroxylysyl-pyridinoline (HP), lysyl-pyridinoline (LP), and pentosidine (PE). After drying the specimen at 21 °C in a vacuum oven (25 in Hg), the mass of the small piece was measured with a precision microbalance (UMX2, Mettler Toledo, Greifensee, Switzerland). The sample was then hydrolyzed in 500 μ L of 6 N HCl at 110 °C for at least 20 hours, and the hydrolysate was split into two disposable culture tubes (at a

nominal ratio of 50:50). The residue of one split sample was re-suspended with a known volume (400 μL) of ultra-pure water plus a dissolved internal standard (94.2 μM pyridoxine). Next, following a method described by Bank et al.,³⁵ the concentration of HP, LP, and PE was determined using high performance liquid chromatography (HPLC). The crosslink concentrations of each specimen were then normalized by its respective collagen content (Col), as determined by a micro-hydroxyproline (Hyp) assay on the remaining sample. For this latter analysis, we used the colorimetric technique that is described by Morales et al.³⁶

Statistical Analysis

The effect of age on the properties of bone (mechanical, morphological, and compositional) was tested (Table 2) using a re-sampling technique called bootstrap (MULTTEST Procedure, SAS/STAT User's Guide version 9, 2004, SAS Institute Inc., Cary, NC). There are several advantages to this technique. One, it does not assume any parametric form for the data (i.e., normality is not necessary).³⁷ Two, it provides a strong estimate of the p-value for small sample sizes (i.e., increases the power of the tests).³⁸ Three, the estimate is more conservative than that given by Student's t-test, which is also calculated by MULTTEST.

Significant associations among the properties were determined by Pearson's correlation coefficients (ρ_{xy}) at $\alpha = 0.05$. To determine which morphological property and compositional properties of bone best explained a mechanical property (irrespective of age group), general linear models were developed (GLM Procedure, SAS/STAT User's Guide version 9, 2004, SAS Institute Inc., Cary, NC). Initially, a model was created to include any morphological and compositional property as an independent factor if it was significantly associated with the mechanical property being analyzed (Table 3). Also, the GLM initially included interactions when the independent factors were significantly associated to one another. Non-significant interactions and factors with the highest p-value were sequentially removed from the model to obtain the highest possible R^2 value.³⁹ Moreover, a similar process was performed but without the intercept term (a_0) to see if this increased the R^2 . All final models had a p-value < 0.005 . Note that there were not enough specimens to include additional bone properties and age in the models (i.e., the power of the test would be too low).

RESULTS

Except for Young's modulus, age affected all other mechanical properties of bone (Table 2) as determined by the progressive, repetitive loading scheme in tension (Fig. 1). Since initial elastic stiffness did not vary between middle and old aged bone, aging apparently affected the capacity of bone to generate damage when overloaded. Age also affected porosity and several compositional properties. Older bone had greater porosity (Po), concentration of pentosidine (PE), mineral density (ρ_m), and water content ($\Delta\text{H}_2\text{O}$) than the younger bone (Table 2). Collagen content (Col), however, decreased with age.

Pearson's analysis revealed that Po, Col, and PE were the only properties that are significantly associated with the post-yield energy terms (i.e., U_{ps} , U_{er} , and U_h) as well as the toughness or the complete energy dissipation (U_T) of bone (Table 3). As to other mechanical properties, Col and PE were the only properties related to the final damage density (D_f), while porosity and water content were correlated with bone strength (Table 3). Giving the highest R^2 value in the GLMs, PE and Col provided the best explanation of the post-yield energy terms, while Po and Col provided the best explanation of bone toughness (Table 4). This is not to say Po does not affect post-yield energy dissipation or PE does not affect toughness. Their contribution to these mechanical properties is just not as dominant when other factors are included. Moreover, a_0 was not statistically significant suggesting a theoretical ratio of PE to Col exists at which there is zero energy dissipation. However, since Col and PE accounted for less than 50% of the variance in U_{ps} , U_{er} , and U_h , other factors are likely involved in determining post-yield

toughness. Among the post-yield energy terms, PE and Col had the greatest contribution to the plastic strain energy (i.e., U_{ps} had the highest coefficients; Table 4).

PE plus a constant (a_0) that could represent an unmeasured variable provided the best explanation of the variance in the D_f (i.e., with no PE, there is still a stiffness loss, and including Col did not improve the explanation), while porosity and ΔH_2O plus an interaction between these two variables provided the best explanation of bone strength (Table 4). The R^2 value for the model of σ_{max} was 99.5% placing certain importance on the volume of water in bone. Such a measure is indicative of the state of porosity and mineralization, two important indicators of strength.⁴⁰ Water tends to fill the pores of ex vivo specimens and mineralization displaces water from collagen.⁴¹

DISCUSSION

While a decline in bone toughness with advancing age has been well reported,¹⁶⁻¹⁹ there is still uncertainty about how structural and compositional changes (at multiple length scales) facilitate this degradation. Older bone appears to be more susceptible to damage accumulation (i.e., microcracks form more readily) than younger bone,¹⁸ and the resistance to crack propagation apparently decreases with an increase in *in vivo* microdamage.⁴² In addition, bone toughness depends on collagen as reviewed by others^{43, 44} and evident when denaturing collagen by heat or enzymes.⁴⁵⁻⁴⁷ Moreover, collagen integrity in bone (as measured by shrinkage temperature) decreases with age.^{48, 49} The question then arises whether age-related changes in collagen allow micro- or nano-cracks in bone to form and propagate more readily. Although the objective of the present study did not attempt to answer these questions, the new measures of post-yield energy dissipation did indicate that age-dependent change in bone quality was strongly associated with collagen. These new measures are potentially related to damage accumulation, viscous behavior, and permanent deformation of bone. In addition, along with fracture toughness characteristics (e.g. R-curve behavior), this approach of partitioning post-yield energy dissipation may prove useful in deducing mechanistic causes for the loss of bone toughness with age.

As observed by Bailey et al.⁵⁰ in trabecular bone, the present study also indicated that age-related decrease in collagen content was associated with a decrease in bone toughness. While this confirms the importance of collagen to the energy dissipation capacity of bone, the measure of collagen content does depend on the degree of mineralization. Following the methods of Bailey et al.,⁵⁰ the collagen assay in the present study was calculated on the dry mass of bone, not on the volume of the organic phase. Thus, the apparent amount of collagen (in mmol per mg of bone tissue) decreases with an increase in mineralization. In fact, we observed that the density of the mineral phase increased with age (Table 2). Furthermore, the mass fraction of mineral did not change with age suggesting that mineral crystals of older bone are closer to each other than younger bone after the removal of the organic phase. While the organic mass fraction of bone does not appear to decrease with age, decreases in collagen content, not increases in mineral density, significantly explained the age-related decrease in the post-yield energy dissipation of bone.

Our observation that mineralization did not relate to the toughness of bone appear contradictory to the findings of Currey et al.^{51, 52} in which an age-related increase in ash fraction was related to a decrease in the work-to-fracture and impact energy of cortical bone. Their study, however, investigated a wider range of ages (8 to 80 years) than the present work, and the difference in mineral content among specimens from older donors (> 50 years) was less than that among specimens from younger donors (< 35 years). In other words, there was an association between toughness and the logarithm of ash fraction over seven decades.⁵² Mineral content in bone depends on remodeling activity and osteocyte viability because each affects the distribution of

mineralization; and when measured on bulk samples, it does not necessarily vary with age, an observation reported by others.^{16, 53} Alternative techniques such as density fraction and back scatter electron microscopy have demonstrated that compartments of highly mineralized bone increase with age^{54, 55} and could be of necrotic origin.⁵⁴ The contribution of hypermineralization to bulk measures of mineral content can be offset by less mineralized tissue compartments, which are present because of ongoing bone remodeling. Porosity at the microscopic level can be another confounding factor if the mineral mass is normalized by wet mass (ash fraction) because water fills the pores of *ex vivo* specimens thus adding apparent mass.

With regards to bone strength, mineral mass per dry mass was not significantly correlated (although for $M_{\text{Min}}/M_{\text{wet}}$ versus σ_{max} , ρ_{xy} equaled 0.480 with a p-value of 0.054). On the other hand, ΔH_2O did correlate with strength (Table 3). In the present study, Po was a strong determinant of strength, and by decoupling mineral fraction from Po (i.e., normalizing by dry mass), mineral was not a determinant. Yet, it may have an indirect contribution because ΔH_2O was marginally related to $M_{\text{Min}}/M_{\text{dry}}$ ($\rho_{xy} = -0.458$; p-value = 0.0681) and ΔH_2O did negatively contribute to bone strength through an interaction with Po (Table 4).

Pentosidine, a marker for non-enzymatic crosslinks, may prove useful in assessing bone quality. While relatively low in concentration compared to other advanced glycation end-products,⁵⁶ pentosidine is readily quantifiable and presently associated with age-related decreases in the post-yield energy dissipation of cortical bone. PE and porosity were both related to U_T , U_{ps} , U_{er} , and U_h (Table 3). Yet, Po was found to provide a better explanation of bone toughness or U_T than PE, while the GLMs suggested that the variance in the post-yield energy terms was better explained by the inclusion of PE, not Po. The inclusion of one factor of another in such models do occur when the factors are correlated, which Po and PE were ($\rho_{xy} = 0.529$; p-value = 0.029), and their interaction is not significant. These findings by the GLMs suggest that adding recovered elastic strain energy and final energy to the post-yield energy capacity of bone (Fig. 1) emphasizes Po over PE. Perhaps this is to be expected since Po affects elastic behavior as well as post-yield behavior.¹⁶

There is some question as to whether NEG crosslinks are mechanistically involved in the degradation of bone toughness. Two independent studies did not find that inducing NEG crosslinks by incubating bone in Ribose or Glucose solutions affected the toughness of mineralize bone.^{57, 58} However, Vashishth et al.⁵⁷ did report that non-enzymatic crosslinking decreased the damage fraction, defined as a ratio of secant modulus over initial elastic modulus, of bone. In concurrence, the GLM analysis found that an increase in PE was the best explanatory variable (among the bone properties measured) of the age-related decrease in damage density (Table 4). Perhaps, the role of NEG crosslinks in the toughness of bone involves affecting the stiffness loss mechanism of bone.

Fatigue loading of canine femurs at the mid-diaphysis⁵⁹ and at the femoral neck⁶⁰ caused stiffness loss and strength with an accumulation of damage. The appearance of diffuse damage or microcracks during the cyclic loading or monotonic testing of bone coincides with yielding.^{18, 61} Assuming then that the stiffness loss due to yielding in the present study is reflective of damage accumulation, the capacity to incur damage is greater in younger bone than the older bone. In other words, a lower threshold of damage density may exist for elderly bone, thus causing fracture at lower strain compared with the middle aged bone. This is reflected by the fewer number of surviving specimens in elder bone as deformation increases (Fig. 2).

Because the organization of bone is hierarchical, contributions to toughness exist at multiple length scales and perhaps a number of mechanical measures are necessary to deduce the mechanistic causes in the age-related degradation of bone quality. At the microstructural level,

microcracking,⁶² diffuse damaging,⁶³ and uncracked ligament bridging⁶⁴ have been suggested as toughening mechanisms of bone. Aging may affect these mechanisms at the ultrastructural organization of lamellae or the microstructural organization of cement lines.⁶⁵ There are also studies suggesting that toughness arises at the nano-level in the form of calcium-mediated sacrificial bonds⁶⁶ and a non-fibrillar organic matrix bonding between neighboring mineralized fibrils.⁶⁷ Toughness is the energy required to break these bonds, and this toughness increases with an increase in Ca^{2+} concentration, suggesting ionic attractions hold collagen and mineral together. Whether these mechanisms hold in intact bone is not clear, and may only be of importance when damage forms. Post-yield energy dissipation may prove useful in understanding the mechanisms of age-related loss of bone toughness at multiple length scales.

The number of specimens examined did not allow for examination of the role of age-related interactions on bone toughness. Moreover, the limited age range and the examination of one anatomical site preclude an expansive conclusion on the importance of collagen to fracture risk. Nonetheless, we demonstrate that age-related changes in porosity, non-enzymatic crosslinks (via pentosidine), and collagen content can contribute to the post-yield energy dissipation of bone. The energy dissipation terms are highly interdependent ($\rho_{xy} > 0.97$) and are related to final damage density ($\rho_{xy} \cong 0.92$) and strength ($\rho_{xy} \cong 0.63$). They may be useful in understanding how damage accumulation and collagen interact and contribute to the toughness of bone.

ACKNOWLEDGEMENTS

A grant from NIH/NIA (1 R01 AG022044-01) and from the San Antonio Area Foundation supported the work of the present study.

REFERENCES

1. Schnitzler CM. Bone quality: a determinant for certain risk factors for bone fragility. *Calcif Tissue Int* 1993;53(Suppl 1):S27–S31. [PubMed: 8275376]
2. van der Meulen MC, Jepsen KJ, Mikic B. Understanding bone strength: size isn't everything. *Bone* 2001;29:101–104. [PubMed: 11502469]
3. Schuit SC, van der Klift M, Weel AE, et al. Fracture incidence and association with bone mineral density in elderly men and women: the Rotterdam Study. *Bone* 2004;34:195–202. [PubMed: 14751578]
4. Crabtree NJ, Kroger H, Martin A, et al. Improving risk assessment: hip geometry, bone mineral distribution and bone strength in hip fracture cases and controls. The EPOS study. *European Prospective Osteoporosis Study. Osteoporos Int* 2002;13:48–54. [PubMed: 11883408]
5. Pulkkinen P, Partanen J, Jalovaara P, et al. Combination of bone mineral density and upper femur geometry improves the prediction of hip fracture. *Osteoporos Int* 2004;15:274–280. [PubMed: 14760516]
6. Ahlborg HG, Nguyen ND, Nguyen TV, et al. Contribution of hip strength indices to hip fracture risk in elderly men and women. *J Bone Miner Res* 2005;20:1820–1827. [PubMed: 16160739]
7. Ott SM. When bone mass fails to predict bone failure. *Calcif Tissue Int* 1993;53(Suppl 1):S7–S13. [PubMed: 8275383]
8. Marshall D, Johnell O, Wedel H. Meta-analysis of how well measures of bone mineral density predict occurrence of osteoporotic fractures. *Bmj* 1996;312:1254–1259. [PubMed: 8634613]
9. Petersen MM, Jensen NC, Gehrchen PM, et al. The relation between trabecular bone strength and bone mineral density assessed by dual photon and dual energy X-ray absorptiometry in the proximal tibia. *Calcif Tissue Int* 1996;59:311–314. [PubMed: 8781060]
10. Augat P, Reeb H, Claes LE. Prediction of fracture load at different skeletal sites by geometric properties of the cortical shell. *J Bone Miner Res* 1996;11:1356–1363. [PubMed: 8864911]

11. Cheng XG, Lowet G, Boonen S, et al. Prediction of vertebral and femoral strength in vitro by bone mineral density measured at different skeletal sites. *J Bone Miner Res* 1998;13:1439–1443. [PubMed: 9738516]
12. Aspray TJ, Prentice A, Cole TJ, et al. Low bone mineral content is common but osteoporotic fractures are rare in elderly rural Gambian women. *J Bone Miner Res* 1996;11:1019–1025. [PubMed: 8797124]
13. Xiaoge D, Eryuan L, Xianping W, et al. Bone mineral density differences at the femoral neck and Ward's triangle: a comparison study on the reference data between Chinese and Caucasian women. *Calcif Tissue Int* 2000;67:195–198. [PubMed: 10954772]
14. De Laet CE, Van Hout BA, Burger H, et al. Hip fracture prediction in elderly men and women: validation in the Rotterdam study. *J Bone Miner Res* 1998;13:1587–1593. [PubMed: 9783547]
15. Kanis JA, Johnell O, Oden A, et al. Ten year probabilities of osteoporotic fractures according to BMD and diagnostic thresholds. *Osteoporos Int* 2001;12:989–995. [PubMed: 11846333]
16. McCalden RW, McGeough JA, Barker MB, et al. Age-related changes in the tensile properties of cortical bone. The relative importance of changes in porosity, mineralization, and microstructure. *J Bone Joint Surg Am* 1993;75:1193–1205. [PubMed: 8354678]
17. Burstein AH, Reilly DT, Martens M. Aging of bone tissue: mechanical properties. *J Bone Joint Surg Am* 1976;58:82–86. [PubMed: 1249116]
18. Zioupos P, Currey JD. Changes in the stiffness, strength, and toughness of human cortical bone with age. *Bone* 1998;22:57–66. [PubMed: 9437514]
19. Wang X, Shen X, Li X, et al. Age-related changes in the collagen network and toughness of bone. *Bone* 2002;31:1–7. [PubMed: 12110404]
20. Bonfield, W.; Behiri, JC. Fracture toughness of natural composites with reference to cortical bone. In: Klaus, F., editor. *Application of fracture mechanics to composite materials*. Elsevier; New York: 1989. p. 615-635.
21. Norman TL, Nivargikar SV, Burr DB. Resistance to crack growth in human cortical bone is greater in shear than in tension. *J Biomech* 1996;29:1023–1031. [PubMed: 8817369]
22. Brown CU, Yeni YN, Norman TL. Fracture toughness is dependent on bone location--a study of the femoral neck, femoral shaft, and the tibial shaft. *J Biomed Mater Res* 2000;49:380–389. [PubMed: 10602071]
23. Phelps JB, Hubbard GB, Wang X, et al. Microstructural heterogeneity and the fracture toughness of bone. *J Biomed Mater Res* 2000;51:735–741. [PubMed: 10880123]
24. Yeni YN, Brown CU, Norman TL. Influence of bone composition and apparent density on fracture toughness of the human femur and tibia. *Bone* 1998;22:79–84. [PubMed: 9437517]
25. Yeni YN, Norman TL. Calculation of porosity and osteonal cement line effects on the effective fracture toughness of cortical bone in longitudinal crack growth. *J Biomed Mater Res* 2000;51:504–509. [PubMed: 10880095]
26. Nalla RK, Kruzic JJ, Kinney JH, et al. Effect of aging on the toughness of human cortical bone: evaluation by R-curves. *Bone* 2004;35:1240–1246. [PubMed: 15589205]
27. Ural A, Vashishth D. Cohesive finite element modeling of age-related toughness loss in human cortical bone. *J Biomech*. 2006In press
28. Yang QD, Cox BN, Nalla RK, et al. Fracture length scales in human cortical bone: the necessity of nonlinear fracture models. *Biomaterials* 2006;27:2095–2113. [PubMed: 16271757]
29. Fondrk MT, Bahniuk EH, Davy DT. A damage model for nonlinear tensile behavior of cortical bone. *J Biomech Eng* 1999;121:533–541. [PubMed: 10529922]
30. Jepsen KJ, Davy DT. Comparison of damage accumulation measures in human cortical bone. *J Biomech* 1997;30:891–894. [PubMed: 9302611]
31. Morgan EF, Lee JJ, Keaveny TM. Sensitivity of multiple damage parameters to compressive overload in cortical bone. *J Biomech Eng* 2005;127:557–562. [PubMed: 16121524]
32. Wang X, Nyman JS. A novel approach to assess post-yield energy dissipation of bone in tension. *J Biomech*. 2006In press
33. Lemaitre J, Dufailly J. Damage measurements. *Engineering Fracture Mechanics* 1987;28:643–661.
34. Nyman JS, Roy A, Shen X-m, et al. The influence of water removal on the strength and toughness of cortical bone. *J Biomech* 2006;39:931–938. [PubMed: 16488231]

35. Bank RA, Beekman B, Verzijl N, et al. Sensitive fluorimetric quantitation of pyridinium and pentosidine crosslinks in biological samples in a single high-performance liquid chromatographic run. *J Chromatogr B Biomed Sci Appl* 1997;703:37–44. [PubMed: 9448060]
36. Morales TI, Woessner JF, Howell DS, et al. A microassay for the direct demonstration of collagenolytic activity in Graafian follicles of the rat. *Biochim Biophys Acta* 1978;524:428–434. [PubMed: 208623]
37. Westfall, PH.; Tobias, RD.; Rom, D., et al. *Multiple Comparisons and Multiple Tests Using SAS*. SAS Institute, Inc; Cray: 1999.
38. Chernick, MR. *Bootstrap Methods: A Practitioner's Guide*. John Wiley & Sons; New York: 1999.
39. Little, RC.; Stroup, WW.; J., FR. *SAS for Linear Models*. SAS Institute Inc; Cary: 2002.
40. Hernandez CJ, Beaupre GS, Keller TS, et al. The influence of bone volume fraction and ash fraction on bone strength and modulus. *Bone* 2001;29:74–78. [PubMed: 11472894]
41. Robinson RA. Physiocochemical structure of bone. *Clin Orthop* 1975;112:263–315. [PubMed: 1192643]
42. Norman TL, Yeni YN, Brown CU, et al. Influence of microdamage on fracture toughness of the human femur and tibia. *Bone* 1998;23:303–306. [PubMed: 9737354]
43. Vashishth D. Age-dependent biomechanical modifications in bone. *Crit Rev Eukaryot Gene Expr* 2005;15:343–358. [PubMed: 16472064]
44. Burr DB. The contribution of the organic matrix to bone's material properties. *Bone* 2002;31:8–11. [PubMed: 12110405]
45. Wang X, Bank RA, TeKoppele JM, et al. Effect of collagen denaturation on the toughness of bone. *Clin Orthop* 2000;371:228–239. [PubMed: 10693570]
46. Wang X, Bank RA, TeKoppele JM, et al. The role of collagen in determining bone mechanical properties. *J Orthop Res* 2001;19:1021–1026. [PubMed: 11781000]
47. Wang X, Li X, Bank RA, et al. Effects of collagen unwinding and cleavage on the mechanical integrity of the collagen network in bone. *Calcif Tissue Int* 2002;71:186–192. [PubMed: 12200651]
48. Zioupos P, Currey JD, Hamer AJ. The role of collagen in the declining mechanical properties of aging human cortical bone. *J Biomed Mater Res* 1999;45:108–116. [PubMed: 10397964]
49. Danielsen CC, Mosekilde L, Bollerslev J, et al. Thermal stability of cortical bone collagen in relation to age in normal individuals and in individuals with osteoporosis. *Bone* 1994;19:91–96. [PubMed: 8024858]
50. Bailey AJ, Sims TJ, Ebbesen EN, et al. Age-related changes in the biochemical properties of human cancellous bone collagen: relationship to bone strength. *Calcif Tissue Int* 1999;65:203–210. [PubMed: 10441651]
51. Currey JD. Changes in the impact energy absorption of bone with age. *J Biomech* 1979;12:459–469. [PubMed: 457700]
52. Currey JD, Brear K, Zioupos P. The effects of ageing and changes in mineral content in degrading the toughness of human femora. *J Biomech* 1996;29:257–260. [PubMed: 8849821]
53. Zioupos P. Ageing human bone: factors affecting its biomechanical properties and the role of collagen. *J Biomater Appl* 2001;15:187–229. [PubMed: 11261600]
54. Boyce TM, Bloebaum RD. Cortical aging differences and fracture implications for the human femoral neck. *Bone* 1993;14:769–778. [PubMed: 8268051]
55. Simmons ED Jr, Pritzker KP, Grynblas MD. Age-related changes in the human femoral cortex. *J Orthop Res* 1991;9:155–167. [PubMed: 1992064]
56. Knott L, Bailey AJ. Collagen cross-links in mineralizing tissues: a review of their chemistry, function, and clinical relevance. *Bone* 1998;22:181–187. [PubMed: 9514209]
57. Vashishth D, Gibson GJ, Khoury JI, et al. Influence of nonenzymatic glycation on biomechanical properties of cortical bone. *Bone* 2001;28:195–201. [PubMed: 11182378]
58. Reddy GK. Glucose-mediated in vitro glycation modulates biomechanical integrity of the soft tissues but not hard tissues. *J Orthop Res* 2003;21:738–743. [PubMed: 12798076]
59. Burr DB, Turner CH, Naick P, et al. Does microdamage accumulation affect the mechanical properties of bone? *J Biomech* 1998;31:337–345. [PubMed: 9672087]

60. Hoshaw SJ, Cody DD, Saad AM, et al. Decrease in canine proximal femoral ultimate strength and stiffness due to fatigue damage. *J Biomech* 1997;30:323–329. [PubMed: 9074999]
61. Zioupos P, Currey JD, Sedman AJ. An examination of the micromechanics of failure of bone and antler by acoustic emission tests and Laser Scanning Confocal Microscopy. *Med Eng Phys* 1994;16:203–212. [PubMed: 8061906]
62. Vashishth D, Tanner KE, Bonfield W. Experimental validation of a microcracking-based toughening mechanism for cortical bone. *J Biomech* 2003;36:121–124. [PubMed: 12485646]
63. Parsamian GP, Norman TL. Diffuse damage accumulation in the fracture process zone of human cortical bone specimens and its influence on fracture toughness. *J Mater Sci Mater Med* 2001;12:779–783. [PubMed: 15348224]
64. Nalla RK, Kruzic JJ, Ritchie RO. On the origin of the toughness of mineralized tissue: microcracking or crack bridging? *Bone* 2004;34:790–798. [PubMed: 15121010]
65. Akkus O, Yeni YN, Wasserman N. Fracture mechanics of cortical bone tissue: a hierarchical perspective. *Crit Rev Biomed Eng* 2004;32:379–426. [PubMed: 15658930]
66. Thompson JB, Kindt JH, Drake B, et al. Bone indentation recovery time correlates with bond reforming time. *Nature* 2001;414:773–776. [PubMed: 11742405]
67. Fantner GE, Hassenkam T, Kindt JH, et al. Sacrificial bonds and hidden length dissipate energy as mineralized fibrils separate during bone fracture. *Nat Mater* 2005;4:612–616. [PubMed: 16025123]
68. Yeni YN, Brown CU, Wang Z, et al. The influence of bone morphology on fracture toughness of the human femur and tibia. *Bone* 1997;21:453–459. [PubMed: 9356740]

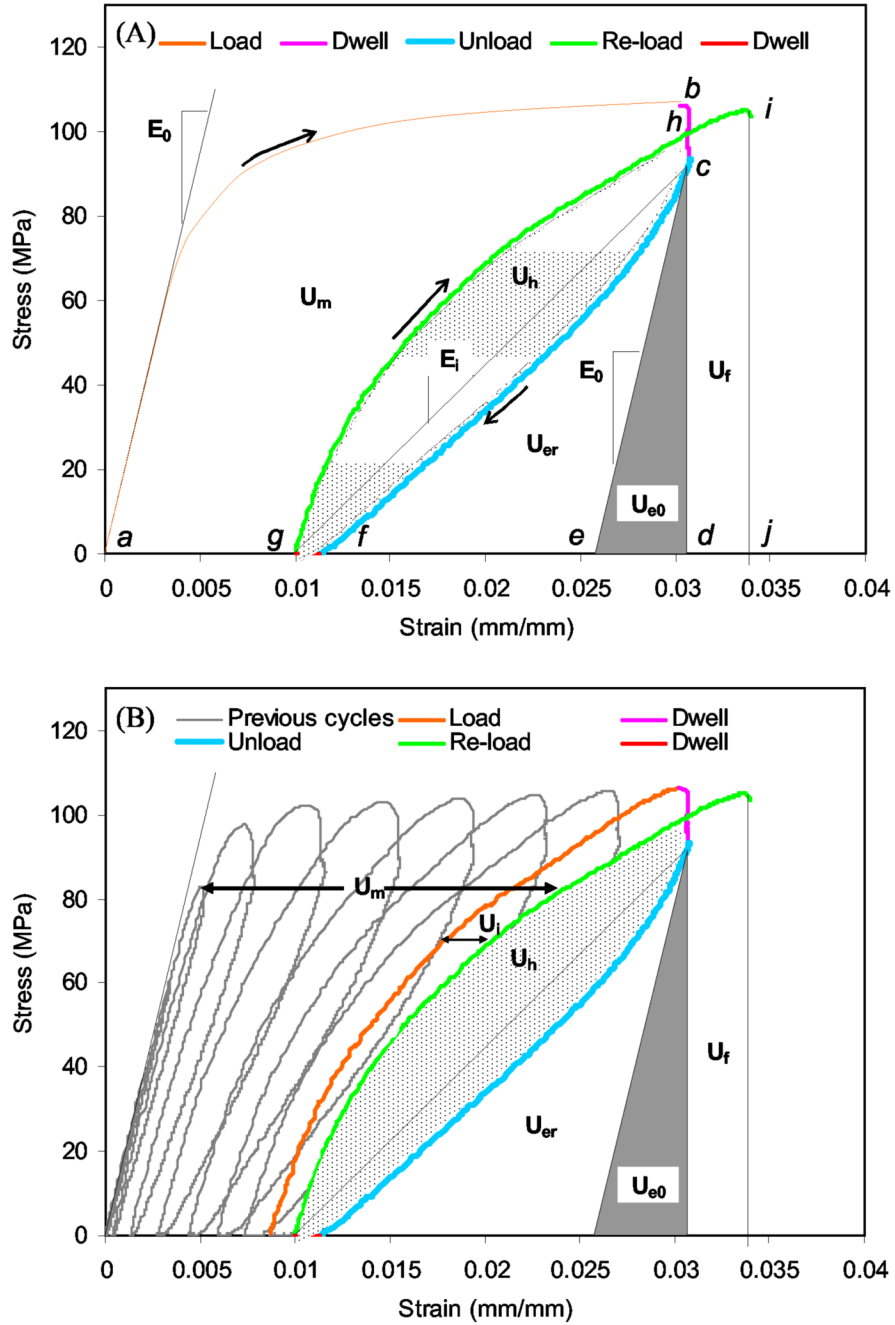


Figure 1. A loading-unloading-reloading scheme with rest insertion (dwell) was used to partition the post-yield energy dissipation of bone (A), but since the failure point was not known, a progressive yield scheme was used and the energies quantified at the last cycle (B).

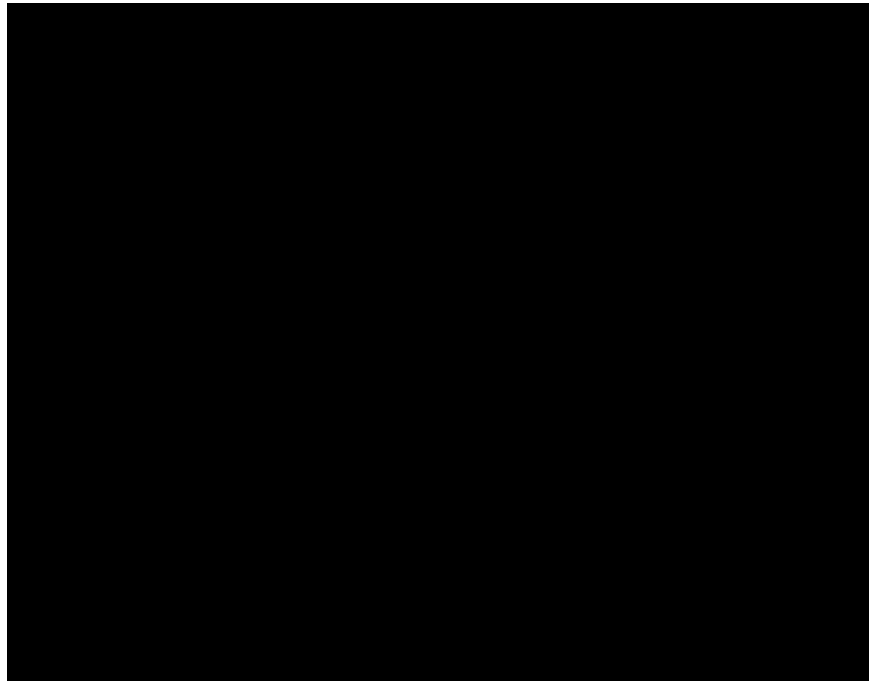


Figure 2.
The number of surviving specimens per total number for old aged bone decreases at lower strain than does middle aged bone.

Table 1

A number of age-related changes in cortical bone properties could potentially affect the quality of bone.

Change in bone property		Association to bone quality		Reference
collagen strength	↓	work-to-fraction	↓	19
pentosidine	↑	collagen strength	↓	19
shrinkage temperature of collagen	↑	work-to-fracture	↓	48
microscopic porosity	↑	post-yield toughness	↓	16
hypermineralized compartments	↑	damaged sites	↓	54
microdamage	↑	work-to-fracture	↓	48
microdamage	↑	resistance to crack propagation	↓	42
interstitial to osteonal hardness ratio	↑	resistance to crack propagation	↓	23
porosity	↑	resistance to crack propagation	↓	24
osteonal areay	↑	resistance to crack propagation	↓	68
water loss by drying	↑	resistance to crack propagation	↓	24

Table 2 There were a number age-related differences in the mechanical, compositional, and morphological properties of bone (mean \pm standard deviation).

Type	Property	Unit	Middle age	Old age	p-value ^d
Morphological	Po	%	10.8 \pm 2.3	16.8 \pm 4.9	0.0018
	PE	mmol/mol	0.316 \pm 0.111	0.537 \pm 0.101	0.0002
Composition	LP	mol/mol	0.104 \pm 0.023	0.108 \pm 0.023	NS ^b
	HP	mol/mol	0.173 \pm 0.031	0.192 \pm 0.023	NS
	HP/LP	-	1.699 \pm 0.278	1.815 \pm 0.207	NS
	Col	mmol/mg	0.678 \pm 0.035	0.611 \pm 0.067	0.0084
	Pb	g/cm ³	2.0 \pm 0.0	2.0 \pm 0.0	NS
	Pm	g/cm ³	3.31 \pm 0.14	3.50 \pm 0.15	0.0089
	M _{Min} /M _{dry}	-	0.681 \pm 0.009	0.675 \pm 0.008	NS
	M _{Org} /M _{wet}	-	0.269 \pm 0.799	0.268 \pm 0.569	NS
	M _{Min} /M _{Org}	-	2.14 \pm 0.09	2.08 \pm 0.08	NS
	Δ H ₂ O	%	31.5 \pm 2.8	34.7 \pm 3.3	0.0241
Mechanical	D _f	-	0.7 \pm 0.1	0.6 \pm 0.1	<0.0001
	U _h	MI/m ³	0.507 \pm 0.161	0.225 \pm 0.052	0.0002
	U _{res}	MI/m ³	0.858 \pm 0.208	0.351 \pm 0.086	<0.0001
	U _{er}	MI/m ³	0.498 \pm 0.166	0.194 \pm 0.059	0.0001
	U _m	MI/m ³	1.356 \pm 0.368	0.546 \pm 0.143	<0.0001
	U _{i=CF}	MI/m ³	0.252 \pm 0.049	0.187 \pm 0.049	0.0082
	U _{a0}	MI/m ³	0.224 \pm 0.027	0.185 \pm 0.020	0.0028
	U _T	MI/m ³	2.73 \pm 0.73	1.36 \pm 0.34	0.0002
	σ_{max}	MPa	104.9 \pm 8.2	96.8 \pm 6.2	0.0177
	E ₀	GPa	18.5 \pm 1.5	18.2 \pm 1.4	NS

^a One-tail test of significance

^b Not statistically significant

Table 3

Pearson's correlation coefficients (ρ_{xy}) reveal several statistically significant associations between the mechanical properties and compositional properties of bone ($n = 17$). Shading and bold indicate a p-value < 0.05 .

	U_{er}	U_p	U_h	D_f	U_T	σ_{max}
Po	-0.495	-0.510	-0.484	-0.343	-0.486	-0.671
Col	0.559	0.578	0.553	0.606	0.507	0.265
HP	0.052	-0.046	0.048	-0.099	0.094	0.266
LP	0.088	0.078	0.084	0.058	0.146	0.104
PE	-0.652	-0.671	-0.662	-0.649	-0.602	-0.466
HP/LP	-0.078	-0.152	-0.078	-0.165	-0.121	0.088
ρ_b	0.000	0.062	-0.014	-0.151	0.007	0.385
ρ_m	-0.387	-0.385	-0.376	-0.335	-0.315	-0.288
M_{Min}/M_{dry}	0.011	0.075	0.000	0.0266	0.0167	0.257
M_{Org}/M_{wet}	0.243	0.178	0.252	0.064	0.194	0.163
M_{Min}/M_{Org}	0.008	0.070	-0.004	0.027	0.013	0.254
ΔH_2O	-0.312	-0.301	-0.311	-0.134	-0.257	-0.493

The best explanatory and age-related variables for selected mechanical properties of bone were determined from GLMs with the highest R^2 value and significant coefficients (a_i).

Table 4

Property	Intercept ^a		P ₀		PE		Col		R ²
	a_0	p-value	a_1	p-value	a_2	p-value	a_3	p-value	
U _{er}	NI ^b	NI	NI	NI	-0.612	0.0108	0.946	<0.0001	46.8
U _{ps}	NI	NI	NI	NI	-0.939	0.0083	1.568	<0.0001	49.7
U _h	NI	NI	NI	NI	-0.567	0.0108	0.946	<0.0001	47.3
U _T	NI	NI	-0.0830	0.0309	NI	NI	4.993	<0.0001	40.1
D _f	0.838	<0.0001	NI	NI	-0.411	0.0048	NI	NI	42.1
Property	Intercept		P ₀		ΔH_2O		P ₀ * ΔH_2O		R ²
σ_{max}	a_0	p-value	a_1	p-value	a_2	p-value	a_3	p-value	99.5
	NI	NI	7.635	0.0008	3.598	<0.0001	-0.265	<0.0001	

^a Represents an unmeasured variable.

^b Terms were not included (NI) because their contribution was not significant and their inclusion lowered the R^2 value.